Holographic Software for Quantum Networks

Arthur Jaffe,[*] Zhengwei Liu,[†] and Alex Wozniakowski[‡]

Harvard University, Cambridge, MA 02138, USA

We introduce diagrammatic protocols and holographic software for quantum information and quantum simulation. We give a dictionary to translate between diagrammatic protocols and the usual algebraic protocols. In particular we describe the intuitive diagrammatic protocol for teleportation. We introduce the string Fourier transform $\mathfrak{F}_s$ in quantum information, which gives a topological quantum computer. We explain why the string Fourier transform maps the zero particle state to the multipartite entangled state, which maximizes the entanglement entropy. We construct a multipartite protocol that generalizes BVK. We study Pauli X, Y, Z matrices, and their relation with diagrammatic protocols. This work provides bridges between the new theory of planar para algebras and quantum information, especially in questions involving communication in quantum networks.

CONTENTS

[*] arthur_jaffe@harvard.edu
[†] zhengweiliu@fas.harvard.edu
[‡] airwozz@gmail.com

I. INTRODUCTION

In this paper we introduce holographic diagrammatic software for quantum information, and we illustrate its use. Our software captures two directions of thinking that we describe below: algebra to topology; and topology to algebra. We use the term "holographic," since one can translate any algebraic protocol into diagrams, and we may simplify the algebraic computation using topological isotopy. This describes the direction algebra to topology.
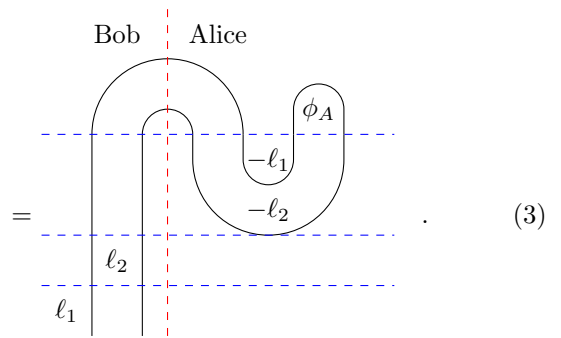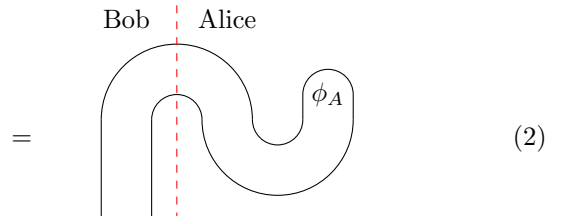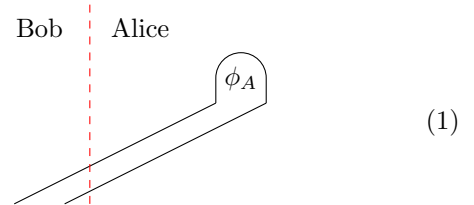
The inverse direction, topology to algebra, is more interesting. In this paper, we recover some fundamental concepts in quantum information by following topological intuition. This philosophy also leads to new concepts and applications. One can introduce diagrammatic protocols and translate them into the usual algebraic protocols using our dictionary of the holographic software. This provides a new framework to explore the efficient simulation of physical systems [1–3].

A. From topology to quantum information: An example

Let us explain our ideas with our favorite example. Suppose that Alice wants to teleport her qudit to Bob. That means that she wants to exchange the location of the qudit without having a quantum communication channel linking her to Bob.

Can we simulate this quantum process by topology? We outline here the ideas of how this works; we explain these ideas in detail later in this paper.

Our diagrammatic protocol given in (1) obviously simulates teleportation from Alice to Bob. However one must ask: does this diagram makes sense in quantum information? The answer is no. The part of the diagram that extends over the dashed red line is a non-local transformation, which cannot be implemented by Alice and Bob in the real world. In other words the diagram in (1) is a noiseless quantum channel linking Alice to Bob, which we assumed was not an available resource in the protocol.

Bob　Alice

$$\phi_A \tag{1}$$

Bob　Alice

$$= \qquad \phi_A \tag{2}$$

Bob　Alice

$$= \qquad \begin{matrix} \phi_A \\ -\ell_1 \\ -\ell_2 \\ \ell_2 \\ \ell_1 \end{matrix} \ . \tag{3}$$

The solution to this problem is to simply make a topological isotopy that deforms the diagram into (2). What is the difference? Now the diagram extending over the red line is on the top of the picture. That means it becomes an entangled resource state, which *can* be realized in our real world.

Actually, entanglement is one of the main features of quantum information; it enables advances in far reaching areas such as security, quantum foundations, and computational complexity.

Is that enough? Not yet. In quantum information, we cannot predict the measurement outcome. That means we may have charges on the cups in the diagram, which indicate the result of the measurement. So one needs to make up the opposite charge on the strings on the left, as shown in (3). That means Alice broadcasts her results classically to Bob, and Bob implements the corresponding transformation to obtain a perfect replica of Alice's unknown quantum state.

Now we have obtained the topological protocol for teleportation. Let us see what we have obtained as a protocol, expressed in terms of the usual algebraic terminology. We do this translation using our holographic software.

First, we obtain a maximally-entangled state, which is the standard resource state.

Secondly, we obtain a measurement outcome, which is measurement in the phase space. In addition, measurement arising in this pictorial way maps pure states to

pure states.

Thirdly, the transformations that arise on the left-hand strings are Pauli X, Y, Z matrices, given in (31).

Therefore we recover from holographic software these fundamental concepts in quantum information. We end up with the original algebraic teleportation protocol, which was identified by Bennett et al [4], and which we illustrate in Figure 1.
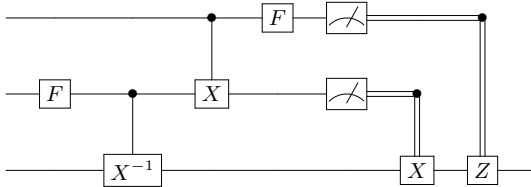

FIG. 1. Algebraic protocol for teleportation.

Instead of presupposing the notions of quantum information, we find that they arise naturally, from following the topological intuition in our model. After defining holographic software in the bulk of our paper, we give more details for this protocol in §IV A.

If we simulate more complicated topological processes, then we find that our holographic software leads to new concepts, as well as new protocols in quantum information.

B. Two philosophies

The mathematical history of understanding the connection between algebra and topology goes back to the early 1900's in the development of homology theory. A quantum version of this philosophy arose thirty years ago when Vaughan Jones found quantum knot invariants [5–7]. In this theory, one gets diagrammatic representations for algebraic identities and topological invariants. This is what we call going from *algebra to topology.*

Jones then asked the question: can these invariants be derived in a topological manner, rather than in an algebraic way? Witten gave a topological interpretation of the Jones polynomial in terms of the Chern-Simons action [8]. Actually Witten's picture is more general. It led to the construction of a 3-d topological quantum field theory (TQFT), see Atiyah [9], that Reshetikhin, Turaev, and Viro formalized mathematically [10, 11]. The point of this story is that 3-d TQFT captures the algebraic axioms of modular tensor categories. As a concrete example, this includes representation categories of quantum groups. This is the direction *topology to algebra.*

In quantum information, one can imagine the same two philosophies. People attempt to simulate quantum information processing, communication, and sensing by using algebra and topology. The direction topology to algebra was established by the pioneering work of Kitaev, Freedman, Larsen, and Wang [12–14].

On the other hand, many people study the topological features of the algebraic model that simulate universal quantum computation and quantum networks.[1] This follows the direction: algebra to topology. Kauffman pointed out the topological features that appear in knot theory [16]. The group of Coecke has made extensive contributions to this approach from the categorical point of view [17–19].

Like the work of Kitaev, our approach captures both philosophies. We start with a topological model constructed in another paper [20]. We design the holographic software using the topological model. In §III we describe how these ideas allow one to design protocols in a new way.

C. Other protocols

In (1) we illustrate our diagrammatic protocol for the standard teleportation. We introduce the multipartite[2] entangled resource state $|\text{Max}\rangle$. One can also construct the resource state by a generalized protocol of Bose, Vedral, and Knight [21] using minimal cost of edits, cdits, and time; see §IV B–§IV C. Our generalized BVK protocol is motivated by [21], as well as the problem of efficiently entangling nodes in a distributed quantum computer or a quantum internet [22].

In another paper [23], we give a new compressed teleportation (CT) protocol involving n-qudits. We discovered this protocol using holographic software. So we believe that the diagrams studied here provide an interesting paradigm for quantum information.

We expect that the CT protocol can be realized for multipartite communication in Pan's space science project [24]. This group plans in the next few months to launch a Quantum Science Satellite for long-distance teleportation [25].

There are many other interesting protocols, for example [26–42], and it would be nice to analyze such protocols using holographic software.

D. String Fourier transform vs. the braid

Originally we had thought that the fundamental way to think about entanglement of qudits lay in the topological properties of the braid, for the braid allows consideration of isotopy in three dimensions. Many other authors have

––––––––

[1] Diagrammatic notation in quantum information theory originated in the quantum circuit model of Deutsch [15], although without the consideration of topology.

[2] In general we use the term multipartite entanglement for entangled states on a Hilbert space composed of multiple subsystems (physics)/ subspaces (math). We use bipartite for two subsystems (Bell states), and tripartite for three subsystems.

done great work using the braid in quantum information, and this is why we give so many references in that direction in §III G.

But after discovering holographic software, we have come to a different understanding. We now believe that the *string Fourier transform* (SFT) that we introduced in [20] provides a robust starting point for many aspects of quantum information, including entanglement. In addition, the SFT gives a topological quantum computer and a universal quantum simulator, thus augmenting the topological model of quantum computation [12–14, 43–45]; see §III J 1.

Our realization of the maximally-entangled, multipartite resource state, as well as our realization of maximal entanglement, is a consequence of the SFT. It comes from the SFT of the zero particle state. The algebraic formulas for the SFT and for the braid can be derived from one another. But we have learned to think about entanglement in terms of the SFT. And this provides insight into computations, and it yields simplification for a number of quantum information protocols; it also suggests new protocols.

Our SFT arose originally in the more general context of planar para algebras, before we understood the depth of its significance for quantum information. Geometrically, the SFT acts on diagrams and gives them a partial rotation. These diagrams might represent qudits, transformations, or measurements.

1. The maximally-entangled multipartite resource state

In this paper we focus on a special subset of SFT's that transform n-qudits to n-qudits. Then the SFT acts as a very interesting unitary transformation $\mathfrak{F}_s$ on the Hilbert space of n-qudits, that has dimension d^n. The transformation $\mathfrak{F}_s$ applied to the n-qudit zero particle state $|\vec{0}\rangle$ creates the n-qudit $|\text{Max}\rangle$. Briefly the standard n-qudit orthonormal basis $|\vec{k}\rangle$ is characterized by a set of charges $\vec{k} = (k_1, \ldots, k_n)$, with values $k_j \in \mathbb{Z}_d$, and with total charge $|\vec{k}| = k_1 + \cdots + k_n$. In §III J 1 we compute the matrix elements of $\mathfrak{F}_s$ and show that

$$|\text{Max}\rangle = \mathfrak{F}_s\,|\vec{0}\rangle = \frac{1}{d^{\frac{n-1}{2}}} \sum_{|\vec{k}|=0} |\vec{k}\rangle . \tag{4}$$

In §III K we discuss definitions of entanglement entropy $\mathcal{E}$, and explain how $|\text{Max}\rangle$ maximizes this entropy. Thus we claim that the qudit $|\text{Max}\rangle$ is a maximally entangled n-qudit. The state $|\text{Max}\rangle$ provides the natural multipartite analog of the Bell state.

We give the diagrammatic representation for $|\text{Max}\rangle$ in Fig. 2. This is the multipartite entangled resource state for our protocols, which we discuss in §IV B, and which we use in our new protocol [23].

When the multipartite entangled state occurs in protocols, we indicate the corresponding n-qudit resource in Fig. 3.
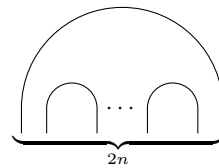

FIG. 2. Diagrammatic representation of the multipartite entangled state $|\text{Max}\rangle$. There are $2n$ output points at the bottom.

FIG. 3. Protocol for $|\text{Max}\rangle$, the multipartite entangled resource state. There are n input and n output lines.

In the special case of order $d = 2$ and $n = 2$ (i.e. for 2-qubits), the matrix $\mathfrak{F}_s$ is the Hadamard transformation, followed by CNOT—the usual way to entangle two qubits—and in this case $|\text{Max}\rangle$ is the Bell state.

E. The relation between $|\text{Max}\rangle$ and $|\text{GHZ}\rangle$

The state

$$|\text{GHZ}\rangle = \frac{1}{d^{\frac{1}{2}}} \sum_{k=0}^{d-1} |k, k, \ldots, k\rangle \tag{5}$$

was considered as a multipartite resource state (originally for n-qubit entanglement) by Greenberger, Horne, and Zeilinger [26]. In §III L we show the entangled states $|\text{GHZ}\rangle$ and $|\text{Max}\rangle$ are related by a local transformation, i.e. by a simple tensor product of transformations. In fact $|\text{GHZ}\rangle$ is the ordinary Fourier transform of $|\text{Max}\rangle$,

$$|\text{GHZ}\rangle = (F \otimes \cdots \otimes F)^{\pm 1}|\text{Max}\rangle , \tag{6}$$

with the Fourier transform F on a single qudit defined in (10).

F. Some other key aspects of holographic software

Let us mention some other key aspects of holographic software that we explain in this paper. These features allow us to give a mosaic of diagrams that represent qudits, measurements, and transformations.

We have made very careful choices of our conventions. For instance we put the charge on the right side of a cap in (28); this corresponds to the choice of q rather than q^{-1} in (11). This also corresponds to the choice of decreasing basis in (36). We believe that it is difficult to change any of our choices, while preserving *all* the beautiful diagrammatic relations that we present here.

- We represent qudits, meters, and transformations as diagrams with input points on the top and output points on the bottom.

- A 1-qudit is a cap; it has zero input points and 2 output points.

- We assign labels to the strings in our diagrams, representing "charge" on the string.

- *Para isotopy* generalizes topological isotopy and allows us to manipulate diagrams with charge.

- The diagram for a twisted product yields insight into para isotopy for charge-neutral subsystems.

- Braids can be defined in terms of planar diagrams and relate to entanglement.

- Charged diagrams can pass freely under our braids, but not over them.

- We obtain elementary diagrams for n-qudit Pauli matrices X, Y, Z.

- We represent local transformations diagrammatically.

- In the case that local transformations are Pauli matrices, one obtains an intuitive representation for the Jordan-Wigner transformation.

We refer persons interested in the mathematical theory behind our diagrams to the paper [20], in which we introduce the notion of "planar para algebras" and analyze them in detail. One also finds an explanation and motivation for the names we use for the diagrammatic relations, as well as proofs of these relations.

G. Does SFT provide quantum simulation?

In classical information theory, the Fourier transform F plays a central role, in particular in signal recovery; see [46] for a robust application. We propose that the SFT could play an analogous role in quantum information.

The question of quantifying the advantage of a quantum computer is a long-standing open problem [47, 48]. The landmark papers of Lloyd [49], Zalka [50], Abrams and Lloyd [51], and Somma et al. [52] provide foundational insights in the pursuit of quantum simulation. In [22, 47, 53, 54] one finds extensive references; experimental work on quantum simulation has been achieved [55–58].

II. BASIC ALGEBRAIC NOTATION

A. Qudits

A 1-qudit is a vector state in a d-dimensional Hilbert space, where d is the *degree* of the qudit. (The usual case of qubits corresponds to $d = 2$.) We denote an orthonormal basis using Dirac notation by $|k\rangle$. We call k

the charge of the qudit, and generally $k \in \mathbb{Z}_d$, the cyclic group of order d.

The dual 1-qudit $\langle \ell |$ is a vector state in the dual space to the d-dimensional Hilbert space. And $\langle \ell | k \rangle = \delta_{\ell,k}$, where $\delta_{\ell k}$ is the Kronecker delta.

The n-qudit space is the n-fold tensor product of the 1-qudit space. An orthonormal basis for n-qudits is $|\vec{k}\rangle = |k_1, k_2, \ldots, k_n\rangle$, where this ket has total charge $|\vec{k}| = k_1 + k_2 + \cdots + k_n$. The dual basis is $\langle \vec{\ell} |$. Every linear transformation on n-qudits can be written as a sum of the d^{2n} homogeneous transformations

$$M_{\vec{\ell},\vec{k}} = |\vec{\ell}\rangle\langle\vec{k}|, \quad \text{with charge} \quad |\vec{k}| - |\vec{\ell}|. \quad (7)$$

The matrix elements of $T = \sum_{\vec{k},\vec{\ell}} t_{\vec{\ell},\vec{k}} \, M_{\vec{\ell},\vec{k}}$ are just $t_{\vec{\ell},\vec{k}} = \langle \vec{\ell} | T | \vec{k} \rangle$.

B. The parafermion algebra

The *parafermion algebra* is a $*$-algebra with unitary generators c_j, which satisfy

$$c_j^d = 1 \quad \text{and} \quad c_j c_k = q \, c_k c_j \quad \text{for} \quad 1 \leqslant j < k \leqslant m. \quad (8)$$

Here $q \equiv e^{\frac{2\pi i}{d}}$, $i \equiv \sqrt{-1}$, and d is the order of the parafermion. Consequently $c_j^* = c_j^{-1} = c_j^{d-1}$, where $*$ denotes the adjoint. Majorana fermions arise for $d = 2$.

The Jordan-Wigner transformation is an isomorphism between the parafermion algebra with $2n$ generators and the n-fold tensor product of the $d \times d$ matrix algebra, the latter gives n-qudit transformations. Therefore, we can express n-qudit transformations as elements in the parafermion algebra.

C. Transformations of 1-qudits

Let $q^d = 1$ and $\zeta = q^{1/2}$ be a square root of q with the property $\zeta^{d^2} = 1$. Matrices X, Y, Z, F, G play an important role. Three of these are the qudit Pauli matrices

$$X|k\rangle = |k+1\rangle, \ Y|k\rangle = \zeta^{1-2k}|k-1\rangle, \ Z|k\rangle = q^k|k\rangle. \quad (9)$$

The Fourier matrix F and the Gaussian G are

$$F|k\rangle = \frac{1}{\sqrt{d}} \sum_{\ell=0}^{d-1} q^{k\ell}|\ell\rangle, \quad G|k\rangle = \zeta^{k^2}|k\rangle. \quad (10)$$

These matrices satisfy the relations

$$XY = qYX, \quad YZ = qZY, \quad ZX = qXZ, \quad (11)$$

$$XYZ = \zeta, \quad FXF^{-1} = Z, \quad GXG^{-1} = Y^{-1}. \quad (12)$$

D. Transformations of 2-qudits

1. The multipartite entangled resource state

We represent the multipartite entangled resource state for 2-qudits as

$$|\text{Max}\rangle = \frac{1}{\sqrt{d}} \sum_{k=0}^{d-1} |k, -k\rangle .$$

We say it costs 1 edit if two persons use this entangled state in a protocol.

2. Controlled gates

We give the protocol for controlled transformations $C_{1,A}$ in Fig. 4 and $C_{A,1}$ in Fig. 5, for different control qudits.
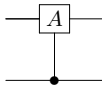
FIG. 4. The controlled gate $C_{1,A}$ acts on the 2-qudit $|k_1, k_2\rangle$ gives $C_{1,A}|k_1, k_2\rangle = |k_1, A^{k_1} k_2\rangle$. The first qudit is the control qudit.
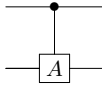
FIG. 5. The controlled gate $C_{A,1}$ acts on the 2-qudit $|k_1, k_2\rangle$ and gives $C_{A,1}|k_1, k_2\rangle = |A^{k_2} k_1, k_2\rangle$. The second qudit is the control qudit.

We sometimes allow more general controlled transformations of the form

$$T = \sum_{l=0}^{d-1} |\ell\rangle\langle\ell| \otimes T(\ell), \tag{13}$$

where the control is on the first qudit, and $T(\ell)$ can be arbitrary on the target qudit. This is shown in Fig. 6; a corresponding configuration with the second control bit would also possible.
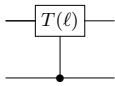
FIG. 6. Controlled transformations.
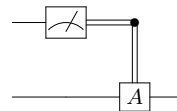
The measurement controlled gate is illustrated in Fig. 7.

FIG. 7. Measurement controlled gate: If the qudit is measured by the meter as k, then they apply A^k to the target qudit. It costs 1 cdit to transmit the result, when the two qudits belong to different persons.

E. Qubit case: $d = 2$ and $\zeta = +i$

In the case $d = 2$ with $\zeta = +i = \sqrt{-1}$ the 1-qubit matrices X, Y, Z are the Pauli matrices $\sigma_x, \sigma_y, \sigma_z$, while $F = H = \frac{1}{\sqrt{2}} \begin{pmatrix} 1 & 1 \\ 1 & -1 \end{pmatrix}$ is the Hadamard matrix, and $G = S = \begin{pmatrix} 1 & 0 \\ 0 & i \end{pmatrix}$ is the phase transformation. For 2-qubits, the transformation $C_{1,X}$ is CNOT. These transformations can be realized efficiently in nature [59–61]. The transformations they generate are local transformations.

F. Simplifying tricks

We give four elementary algebraic tricks to simplify the algebraic protocols; we illustrate them in Figs. 8–11.

FIG. 8. Trick 1: The control gate commutes with the phase transformation on the control qudit.

FIG. 9. Trick 2: The phase transformation does not affect measurement of the meter, so we can remove it.

III. HOLOGRAPHIC SOFTWARE

In this section we give the dictionary to translate between diagrammatic protocols and the algebraic ones. Any algebraic protocol can be translated into a diagrammatic protocol in a straightforward way. From this diagram we may be able to obtain new insights into the protocol.

We also give a dictionary for the inverse direction. Actually this is more interesting, as the diagrams may be more intuitive: one says that 1 picture is worth 1,000 words. In fact we give a new way to design protocols: we rely on the aesthetics of a diagram as motivation for the structure of the protocol. In this way, we can strive to introduce diagrammatic protocols which simulate human thought.
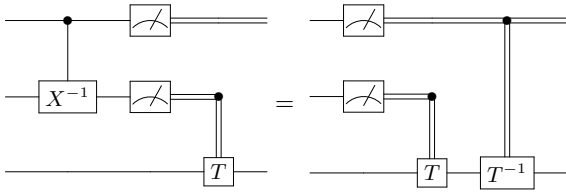
FIG. 10. Trick 3: We can remove the controlled transformation $C_{X,1}^{-1}$ before the double meters by changing the measurement controlled gate.
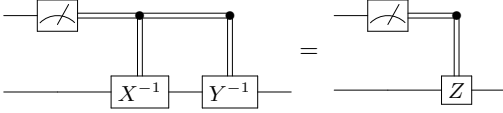

FIG. 11. Trick 4: Since $Y^{-i}X^{-i} = \zeta^{-i^2}Z^i$, and the phase does not count in the protocol, we can simplify meter-controlled transformations.

A. Diagrams for fundamental concepts

Before we give the complete list of diagrammatic relations and our dictionary for translation, let us remark how some fundamental concepts in quantum information fit into our diagrammatic framework.

In §II B we remark that one can write any n-qudit transformation as an element in the parafermion algebra with $2n$ generators. We represent the basis element $c_1^{k_1}c_2^{k_2}\cdots c_{2n}^{k_{2n}}$ in the parafermion algebra as a diagram with $2n$ "through" strings, with the jth string labelled by k_j (on the left side). The label is called the charge of the string, and the labels are positioned in an increasing vertical order:

$$c_1^{k_1}c_2^{k_2}\cdots c_{2n}^{k_{2n}} = \left.\begin{array}{c}\\ k_1\end{array}\right|\left.\begin{array}{c}k_2\\ \end{array}\right|\cdots\left.\begin{array}{c}k_{2n}\\ \end{array}\right| . \tag{14}$$

The algebraic relations (8) to permute the order of factors in the product, become elementary relations between diagrams, that we will give in (17)-(18). Besides these relations mentioned here, we give other diagrammatic relations in §III C and §III G. In addition, we give examples of how to apply these relations to quantum information.

We can also represent n-qudits as diagrams. Perhaps the most important qudit is the zero-particle state $|\vec{0}\rangle$, that we represent (up to a scalar) as a diagram consisting of n caps:

$$d^{n/4}|\vec{0}\rangle = \cap \quad \cap \quad \cdots \quad \cap \quad . \tag{15}$$

The action of the parafermion algebra on the state $|\vec{0}\rangle$ is captured by the joint relations between the charged strings and the caps given in Equations (20).

It is extremely important that the multipartite entangled resource state $|\text{Max}\rangle$ (even in the case of multiple-persons) can be represented as the diagram in Fig. 2. This representation provides new insights in multipartite

communication, which we explain later in this paper, and also in [23].

B. Elementary notions

We use a convention in identifying algebraic formulas with diagrammatic ones: the objects on the left side of an equation are represented by the objects on the right side of the equation.

In our diagrams, we call the points on top *input points*, and the points on bottom *output points*. The multiplication goes from bottom to top, and glues input points to output points. Tensor products go from left to right.

An n-qudit has 0 input points and $2n$ output points. A dual n-qudit has $2n$ input points and 0 output points.

We call a diagram with n input points and n output points an n-string transformation.

An n-qudit transformation is a $2n$-string transformation. (An n-qudit transformation is an n-string transformation in previous diagrammatic approaches, such as in [16, 17].) It is interesting that one can also talk about a 1-string transformation that acts on "$\frac{1}{2}$-qudits". We refer the readers to [23] for an application of this concept.

We call

$$k\left.\right| \tag{16}$$

a k-charged string, or a string with a k-charged particle. We write the label to the left of the string.

C. Planar relations

In this section we give relations between certain diagrams. The consistency of these relations is proved in [20]. Using these relations, we give a dictionary between qudits, transformations and diagrams.

1. Addition of charge, and charge order

$$\left.\begin{array}{c}\ell\\ k\end{array}\right| = k+\ell\left.\right| , \qquad d\left.\right| = \left.\right| . \tag{17}$$

2. Para isotopy

$$\left.\begin{array}{c}\\ k\end{array}\right|\left.\right|\cdots\left.\begin{array}{c}\ell\\ \end{array}\right|\left.\right| = q^{k\ell}\left.\begin{array}{c}k\\ \end{array}\right|\left.\right|\cdots\left.\right|\left.\begin{array}{c}\\ \ell\end{array}\right| . \tag{18}$$

Here the strings between k^{th}-charged and ℓ^{th}-charged strings are not charged. We call $q^{k\ell}$ the twisting scalar.

Notation: The twisted tensor product of pairs interpolates between the two vertical orders of the product. In the twisted product, we write the labels at the same vertical height:

$$k \left|\left|\cdots\right|\ell\right| \equiv \zeta^{-k\ell} \left|\left|\cdots\right|^{\ell}\right|_k$$

$$= \zeta^{k\ell} {}^{k}\left|\left|\cdots\right|_{\ell}\right| . \tag{19}$$

In this case $k, l \in \mathbb{Z}$, and k and $k+d$ yield different diagrams. If the pair is neutral, namely $\ell = -k$, then the twisted tensor product is defined for $k \in \mathbb{Z}_d$. This twisted product was introduced in [62, 63].

3. String Fourier relation

$$k \,\bigcap\, = \zeta^{k^2} \,\bigcap k\,, \tag{20}$$

$$k \,\bigcup\, = \zeta^{-k^2} \,\bigcup k\,. \tag{21}$$

4. Quantum dimension

$$\bigcirc = \sqrt{d}\,. \tag{22}$$

5. Neutrality

$$k\,\bigcirc = 0\,, \quad \text{for } d \nmid k. \tag{23}$$

6. Temperley-Lieb relation

$$\bigcup_{\bigcap} = \Big|\,, \quad \bigcap_{\bigcup} = \Big|\,. \tag{24}$$

Notation: Based on the Temperley-Lieb relation, a string only depends on the end points:

$$\bigcap_{} = \diagup\,, \quad \bigcup_{} = \diagdown\,. \tag{25}$$

7. Resolution of the identity

$$\Big|\quad\Big| = d^{-1/2} \sum_{k=0}^{d-1} \frac{\overset{\frown}{-k}}{\underset{k}{\smile}} . \tag{26}$$

D. 1-Qudit dictionary

Now we give the first diagrammatic translations of the algebraic formulas. It will be evident from the context of the diagram, when a symbol such as k denotes a label, in contrast with $d^{-1/4}$ or $q^{k\ell}$ or ζ^{k^2}, that denote a scalar multiple.

1. Qudit

Our diagram for the qudit $|k\rangle$ is:

$$|k\rangle = d^{-1/4}\,\overset{\frown}{k}\,. \tag{27}$$

In other words, according to our convention,

$$\overset{\frown}{k} = d^{1/4}|k\rangle\,. \tag{28}$$

From now on, if the identification in both directions is clear, we only give one of them.

2. Dual qudit

Our diagram for the dual-qudit $\langle k|$ is:

$$\langle k| = d^{-1/4}\,\underset{-k}{\smile}\,. \tag{29}$$

3. Transformations

Transformations T of 1-qudits are diagrams with two input points and two output points. The identity transformation is

$$I = \Big|\quad\Big|\,.$$

4. Matrix Units

The diagram for the transformation $|k\rangle\langle\ell|$ is

$$|k\rangle\langle\ell| = d^{-1/2}\,\frac{\underset{-\ell}{\smile}}{\overset{\frown}{k}}\,. \tag{30}$$

5. Pauli matrices X, Y, Z

The diagrams for Pauli X, Y, Z are:

$$X = \left| \; 1 \; \right|, \quad Y = \left| \; \text{-1} \; \right| \; \left| \; \right|, \quad Z = \; 1 \; \left| \; \text{-1} \; \right|. \quad (31)$$

E. 1-Qudit properties

In this section we explain why the dictionary is holographic for 1-qudits, and we show how the Pauli X, Y, Z in (31) actually correspond to the usual qudit Pauli matrices.

- Orthogonal Basis:

$$\langle \ell | k \rangle = d^{-1/2} \; \overset{k}{\underset{-\ell}{\left(\begin{array}{c} \end{array}\right)}} = \delta_{\ell k} \; . \quad (32)$$

  Here we use the relations (17), (22), and (23).

- Transformations: The matrix units $|k\rangle\langle\ell|$ are represented as in Equation 30.

Therefore single qudit transformations can be represented as diagrams. On the other hand, Relation (26) indicates that any diagram with two input points and two output points is a single qudit transformation. This gives an elementary dictionary for translation between single qudit transformations and diagrams with two input points and two output points. In general, there is a correspondence between n-qudit transformations and diagrams with $2n$ input points and $2n$ output points.

In this way, the diagrammatic computation is the same as the usual algebraic computation in quantum information.

We introduce better diagrammatic representations for local transformations, so that we can utilize other diagrammatic relations.

- Pauli X, Y, Z Relations: Using the notation for qudits in (28) and (31), one can identify these three 2-string transformations as the Pauli matrices defined in (9).

$$\overset{k}{\underset{1}{\left(\begin{array}{c} \end{array}\right)} = \overset{k+1}{\left(\begin{array}{c} \end{array}\right)}, \quad (33)$$

$$\text{-1} \overset{k}{\left(\begin{array}{c} \end{array}\right)} = \zeta^{1-2k} \overset{k\text{-}1}{\left(\begin{array}{c} \end{array}\right)}, \quad (34)$$

$$1 \overset{k}{\underset{\text{-1}}{\left(\begin{array}{c} \end{array}\right)} = q^k \overset{k}{\left(\begin{array}{c} \end{array}\right)}. \quad (35)$$

The diagrammatic equalities in (33)–(35) are a consequence of the relations (17)–(20).

- Vertical reflection or Adjoint: The vertical reflection of diagrams maps the particle of charge k to the particle of charge $-k$. This involution is an anti-linear, anti-isomorphism of diagrams. It interchanges $|k\rangle$ with $\langle k|$. For qudits or transformations, the vertical reflection is the usual adjoint $*$.

F. n-Qudit dictionary

We mainly discuss the 2-qudit case. One can easily generalize the argument to the case of n-qudits.

1. Elementary dictionary

There are two different ways to represent 2-qudits as diagrams indicated by the arrow.

$$|k_1 k_2\rangle^{\searrow} = \frac{1}{d^{1/2}} \; \overset{k_1}{\left| \; \right|} \quad \overset{k_2}{\left(\; \right|}, \quad (36)$$

or

$$|k_1 k_2\rangle^{\nearrow} = \frac{1}{d^{1/2}} \; \overset{k_1}{\left(\; \right.} \quad \overset{k_2}{\left.\; \right)}. \quad (37)$$

Then two representations give two different dictionaries, but they are unitary equivalent. We fix the first choice $|k_1 k_2\rangle = |k_1 k_2\rangle^{\searrow}$ in our software, since it works out better with concepts in quantum information.

We represent an n-qudit $|\vec{k}\rangle = |k_1, k_2, \cdots, k_n\rangle$ as

$$|\vec{k}\rangle = \frac{1}{d^{n/4}} \; \overset{k_1}{\left| \; \right|} \quad \overset{k_2}{\left(\; \right)} \quad \cdots \quad \overset{k_n}{\left(\; \right)} \quad . \quad (38)$$

We can represent the n-qudit transformation $|\vec{k}\rangle\langle\vec{\ell}| = |k_1, k_2, \cdots, k_n\rangle\langle\ell_1, \ell_2, \cdots, \ell_n|$ as

$$|\vec{k}\rangle\langle\vec{\ell}| = \frac{1}{d^{n/2}} \; \underset{-\ell_1}{\left| \; \right|} \quad \underset{-\ell_2}{\left(\; \right)} \quad \cdots \quad \underset{-\ell_n}{\left(\; \right)} \; \overset{k_1}{\left| \; \right|} \quad \overset{k_2}{\left(\; \right)} \quad \cdots \quad \overset{k_n}{\left(\; \right)} \quad . \quad (39)$$

We denote an n-qudit transformation T as

$$T = \underbrace{\boxed{\begin{array}{c} |\cdots| \\ T \\ |\cdots| \end{array}}}_{2n} \; . \quad (40)$$

In the other direction, any diagram with 0 input points and $2n$-outpoint points is an n-qudit. Any diagram with $2n$ input points and $2n$ outpoint points is an n-qudit transformation.

2. Controlled transformations

Suppose T is a single qudit transformation. Now we give the diagrammatic representation of the controlled transformations $C_{1,T}$ and $C_{T,1}$ in Figs. 4–5.

$$C_{1,T} = \frac{1}{\sqrt{d}} \sum_{k=0}^{d-1} \boxed{T^k} \; , \qquad (41)$$

$$C_{T,1} = \frac{1}{\sqrt{d}} \sum_{k=0}^{d-1} \boxed{T^k} \; . \qquad (42)$$

In particular, $C_Z \equiv C_{Z,1} = C_{1,Z}$, as one sees from its action on the basis $C_Z|k_1, k_2\rangle = q^{k_1 k_2}|k_1, k_2\rangle$. Thus

$$\boxed{C_Z} = \qquad . \qquad (43)$$

3. 1-Qudit transformations on 2-qudits

A 1-qudit transformation T can act on 2-qudits by adding two strings on the left or on the right. We can translate these diagrammatic transformations to algebraic ones as follows:

$$\boxed{T} = 1 \otimes T \; , \qquad (44)$$

$$\boxed{T} = C_Z(T \otimes 1)C_Z^{-1} \; . \qquad (45)$$

Furthermore if T has charge k, then this action equals

$$\boxed{T} = T \otimes Z^k \; . \qquad (46)$$

Note (46) is better than (45), since Z^k and T can be performed locally by two persons.

In general, if T has charge k, then

$$\boxed{T} \qquad (47)$$

$$= \underbrace{1 \otimes \cdots \otimes 1}_{2m} \otimes T \otimes \underbrace{Z^k \otimes \cdots \otimes Z^k}_{2n} \; . \qquad (48)$$

4. Jordan-Wigner transformations

As a particular case of (47), we obtain the qudit Jordan-Wigner transformation for $T = X$, Y, or Z. We give an very intuitive diagrammatic interpretation of this transformation in §III H.

$$\left| 1 \right| \cdots \left| \right| = X \otimes Z \otimes \cdots \otimes Z \; , \qquad (49)$$

$$\text{-1} \left| \right| \cdots \left| \right| = Y \otimes Z^{-1} \otimes \cdots \otimes Z^{-1} \; , \qquad (50)$$

$$1\text{-}1 \left| \right| \cdots \left| \right| = Z \otimes 1 \otimes \cdots \otimes 1 \; . \qquad (51)$$

Equivalently, we can represent Pauli matrices on n-qudits as diagrams.

$$X \otimes 1 \otimes \cdots \otimes 1 = \left| 1\text{-}1 \right| 1 \cdots \text{-}1 \left| 1 \right| , \qquad (52)$$

$$Y \otimes 1 \otimes \cdots \otimes 1 = \text{-1} \left| 1\text{-}1 \right| \cdots 1 \text{-}1 , \qquad (53)$$

$$Z \otimes 1 \otimes \cdots \otimes 1 = 1 \text{-}1 \left| \right| \cdots \left| \right| . \qquad (54)$$

If we work on the increasing basis in Equation 37, then we obtain the following Jordan-Wigner transformation:

$$\left| \right| \cdots \left| 1 \right| = Z^{-1} \otimes \cdots \otimes Z^{-1} \otimes X \; , \qquad (55)$$

$$\left| \right| \cdots \text{-1} \left| \right| = Z \otimes \cdots \otimes Z \otimes Y \; , \qquad (56)$$

$$\left| \right| \cdots \left| 1\text{-}1 \right| = 1 \otimes \cdots \otimes 1 \otimes Z \; . \qquad (57)$$

Equivalently,

$$1 \otimes \cdots \otimes 1 \otimes X = 1 \text{-}1 \cdots 1 \text{-}1 \left| 1 \right| , \qquad (58)$$

$$1 \otimes \cdots \otimes 1 \otimes Y = \text{-1} 1 \cdots \text{-}1 1 \text{-1} , \qquad (59)$$

$$1 \otimes \cdots \otimes 1 \otimes Z = \left| \right| \cdots \left| \right| 1 \text{-}1 . \qquad (60)$$

5. Measurement dictionary I

When a protocol has a meter, and the measurement of this meter is ℓ, it is the same as applying the dual qudit $\langle \ell|$ to the corresponding qudit. In a similar way, if the

measurement of a meter on the jth qudit of an n-qudit is ℓ, then the diagram is

$$
m_j = l \longrightarrow \quad \underbrace{\Big|\Big| \cdots \Big|\Big|}_{2(j-1)} \; \Big({}_{\text{-}\ell} \Big) \; \underbrace{\ell\Big|\text{-}\ell\Big| \cdots \; \ell\Big|\text{-}\ell\Big|}_{2(n-j-1)} \quad . \quad (61)
$$

Conversely, the diagram

$$
\underbrace{\Big|\Big| \cdots \Big|\Big|}_{2(j-1)} \; \Big({}_{\text{-}\ell} \Big) \; \underbrace{\Big|\Big| \cdots \; \Big|\Big|}_{2(n-j-1)} \qquad (62)
$$

means that there is a meter on this j^{th} qudit of an n-qudit, and the measurement is ℓ. Moreover, the result is sent to persons who possess the last $(n - j - 1)$ qudits. Then the persons apply $Z^{-\ell}$ to each of the $(n-j-1)$ target qudits. The corresponding protocol is in Fig. 12. Of course we can not predict the result of the measurement, so the diagrammatic protocol must work for all ℓ.
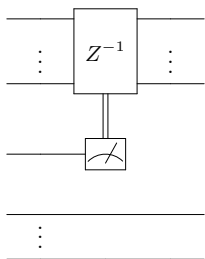

FIG. 12. Measurement controlled-Z gate: If the result of the measurement is k, then one applies Z^k to the target qudits.

G. Braided relations

1. Background

The topological approach to quantum computation became important with Kitaev's 1997 paper proposing an anyon computer—work that only appeared some five years later in print [12]. In §6 on the arXiv, he described the braiding and fusing of anyonic excitations in a fault-tolerant way. Freedman, Kitaev, Larsen, and Wang explored braiding further [13], motivated by the pioneering work of Jones, Atiyah, and Witten on knots and topological field theory [5–9].

In the case $n = 2$, this braid appears in the Jones polynomial. For general n, these braids can be "Baxterized" in the sense of Jones [64]. They are the limits of solutions to the Yang-Baxter equation in statistical physics [65, 66], and have actually been introduced earlier by Fateev and Zamolodchikov [67]. Such kinds of braid statistics in field theory and quantum Hall systems were considered extensively by Fröhlich, see [68, 69]. Fermionic

entanglement was addressed in [70, 71]. Kauffman and Lomonaco remarked that the braid diagram describes maximal entanglement [16]. From our point of view, it is natural to consider entanglement in terms of the string Fourier transform, see §III J 1.

2. The braid

We begin by defining a positive and negative braid in terms of planar diagrams. The braid acts on two strings. The justification for calling this diagram a braid, is that it satisfies the three Reidermeister moves characteristic of a braid. These relations allow one to lift the planar relations to three-dimensional ones. We refer the readers to [20] for the proof of the braided relations stated in this section.

Define $\omega = \frac{1}{\sqrt{d}} \sum_{j=0}^{d-1} \zeta^{j^2}$. Then ω is a phase, as shown in Proposition 2.15 of [20]. Let $\omega^{1/2}$ be a fixed square root of ω. Define the positive braid b_+ as

$$
b_+ = \diagdown\!\!\!\!\diagup \equiv \frac{1}{\sqrt{\omega d}} \sum_{k=0}^{d-1} k \;\Big|{-k}\Big| \qquad (63)
$$

$$
= \frac{1}{\sqrt{\omega d}} \sum_{k=0}^{d-1} \zeta^{k^2} \, k \;\Big|{-k}\Big| \quad .
$$

Here we give two different expressions for the braid. The second formula involves the twisted product given in (19).

The braid is a unitary gate. Its adjoint b_+^* equals the inverse braid, the negative braid $b_+^{-1} = b_-$. In diagrams,

$$
b_+^* = b_- = \diagup\!\!\!\!\diagdown = \frac{\sqrt{\omega}}{\sqrt{d}} \sum_{k=0}^{d-1} k \;\Big|{-k}\Big| \qquad (64)
$$

$$
= \frac{\sqrt{\omega}}{\sqrt{d}} \sum_{k=0}^{d-1} \zeta^{-k^2} \, k \;\Big|{-k}\Big| \quad .
$$

These definitions lead to the following braided relations:

3. Braid-Fourier relation

$$
\mathcal{S} = \diagdown\!\!\!\!\diagup \quad . \qquad (65)
$$

Thus drawing a braid at an arbitrary angle causes no confusion. This equation follows from (18), (21), (26), along with the identity $d^{-1/2} \sum_{k=0}^{d-1} q^{k\ell} \zeta^{k^2} = \omega \zeta^{-\ell^2}$.

4. Reidemeister move I

$$\text{(diagram)} = \omega^{-1/2} \left| \quad \right| \quad . \tag{66}$$

$$\text{(diagram)} = \omega^{1/2} \left| \quad \right| \quad . \tag{67}$$

5. Reidemeister move II

$$\text{(diagram)} = \left| \quad \right| \left| \quad \right| \quad . \tag{68}$$

6. Reidemeister move III

$$\text{(diagram)} = \text{(diagram)} \quad . \tag{69}$$

7. The particle-braid relation

$$\text{(diagram)}_k = \text{(diagram)}_k \quad . \tag{70}$$

This relation demonstrates that any charged diagram can pass freely under (but not over) the braid.

H. Two string braids and local transformations

From the 1-string braid constructed in §III G 2, we obtain a positive and a negative 2-string braid,

$$\text{(diagram)} \quad \text{and} \quad \text{(diagram)} \quad . \tag{71}$$

Theoretically, there are d different 2-string braids. Their actions on 2-qudits are defined by $b_m|k,l\rangle = q^{mkl}|l,k\rangle$, $m \in \mathbb{Z}_d$. Any neutral element can move over and under any two-string braid. Our positive braid is b_{-1} and our negative braid is b_1. Their interpolation b_0 is invariant under the 2-string rotation and adjoint operation, thus we represent this operator as

$$\text{(diagram)} \tag{72}$$

Since $b_0^2 = 1$, we call it a symmetry. We use the symmetry b_0 to swap the order of the qudits. For example, if we want to apply a 2-qudit transformation T to the second and the fourth component of a 5-qudit, then we can represent the transformation diagrammatically as follows,

$$\text{(diagram)} \tag{73}$$

One can generalize this representation for arbitrary cases, meaning any number of qudits and any subsets.

1. Local Transformations

If qudits in the subset belong to one person, then we call the transformation *local*. As examples of local transformations, we recover the Jordan-Wigner transformation for Pauli X, Y, Z in Equations (49),(50),(51) in terms of diagrammatic identities.

2. Jordan-Wigner as Local Transformations

$$\text{(diagram)} \; 1 = \left| 1 \left| \text{-}1 \right| 1 \right| \cdots \left| \text{-}1 \right| 1 \right| , \tag{74}$$

$$\text{(diagram)} \; -1 = \; \text{-}1 \left| \; \right| 1 \left| \text{-}1 \right| \cdots \; 1 \left| \text{-}1 \right| , \tag{75}$$

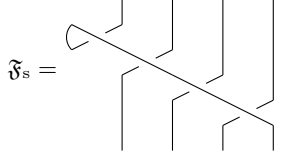$$\text{(diagram)} \; 1 \, \text{-}1 = \; 1 \left| \text{-}1 \right| \; \left| \; \right| \cdots \; \left| \; \right| . \tag{76}$$

I. SFT and maximal entanglement

In [20] we gave a general definition of the string Fourier transform $\mathfrak{F}_s$ on planar diagrams. Analytic properties of SFT have been studied in [72]. Here we analyze the special case of the SFT acting on n-qudits. In this case the transformation is given by a diagram with $2n$ input strings and $2n$ output strings, and it has charge 0. Acting on 2-qudits we illustrate $\mathfrak{F}_s$ in Fig. 13. The diagram for n-qudits is similar. We now analyze the SFT in more detail, both algebraically as well as with some relations for diagrams.

$$\mathfrak{F}_s = \qquad\qquad\qquad\qquad \tag{77}$$

FIG. 13. String Fourier transform on 2-qudits.

1. String Fourier transform $\mathfrak{F}_s$ for 1-qudits

When $n = 1$, we infer from (20), (70), and (66), that

$$\omega^{1/2}\ \diagdown\!\!\!\!\diagup\ = \mathfrak{F}_s = G. \tag{78}$$

The positive and negative braids (63)–(64) also have the representations

$$\diagdown\!\!\!\!\diagup = \frac{\sqrt{\omega}}{\sqrt{d}}\sum_{k=0}^{d-1}\zeta^{-k^2}\ \begin{matrix}\lfloor -k\rceil\\ \lceil k\rfloor\end{matrix}\ , \tag{79}$$

$$\diagup\!\!\!\!\diagdown = \frac{1}{\sqrt{\omega d}}\sum_{k=0}^{d-1}\zeta^{k^2}\ \begin{matrix}\lfloor -k\rceil\\ \lceil k\rfloor\end{matrix}\ . \tag{80}$$

We conclude that $\mathfrak{F}_s$ and the braids act as local transformations on 1-qudits.

2. String Fourier transform $\mathfrak{F}_s$ on 2-qudits

In the $n = 2$ case, $\mathfrak{F}_s$ is a $d^2 \times d^2$ matrix. This matrix is block-diagonal, as it preserves the d different 2-qudit subspaces of fixed total charge, each of dimension d. We call $|0, 0\rangle$ the zero particle state. The string Fourier transformation of the zero particle state is the maximally-entangled, multipartite, resource state

$$\mathfrak{F}_s|0,0\rangle = |\text{Max}\rangle = \frac{1}{\sqrt{d}}\sum_{k=0}^{d-1}|k,-k\rangle\ . \tag{81}$$

The diagrammatic representation of the resource state is in Fig. 14. We use it as a resource to connect diagrams belonging to two persons in a quantum network. In a communication protocol between Alice and Bob, only strings of the resource state are allowed to connect them. Using the resource state costs 1 edit.
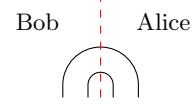

Bob $\quad$ Alice

FIG. 14. Diagrammatic resource state: Only the strings in the resource state are allowed to pass the red (dashed) line between Alice and Bob. (The red line is only for explanation, not a part of the protocol.)

On 2-qudits, $\mathfrak{F}_s$ is a local transformation,

$$\mathfrak{F}_s = (G^{-1}\otimes G)C_{1,X}^{-1}(F\otimes 1)C_{1,X}\ , \tag{82}$$
$$= C_{X,1}^{-1}(1\otimes F)C_{X,1}(G\otimes G^{-1})\ .$$

Note that $G^{-1}\otimes G$ is identity on 0-charge 2-qudits, so

$$\mathfrak{F}_s|0,0\rangle = C_{1,X}^{-1}(F\otimes 1)|0,0\rangle\ . \tag{83}$$

The right side of this expression is the original formula for the resource state.

We have shown that the negative braid

$$\diagup\!\!\!\!\diagdown$$

acts on a qudit basis $|\ell\rangle$ as a local transformation $\omega^{-1/2}G$. It acts on the second and third strings of a 2-qudit as

$$b_{2,3,-} = \Big|\ \diagup\!\!\!\!\diagdown\ \Big|\ . \tag{84}$$

Then

$$b_{2,3,-} = \omega(1\otimes G^{-1})\mathfrak{F}_s(G^{-1}\otimes 1)$$
$$= \omega C_{1,X}^{-1}(G^{-1}FG^{-1}\otimes 1)C_{1,X}$$
$$= \omega C_{X,1}^{-1}(1\otimes G^{-1}FG^{-1})C_{X,1}\ .$$

Thus $b_{2,3,-}$ is a local transformation.

J. Topological quantum computation

The matrices X, Y, Z, F, G generate the 1-qudit Clifford group. The string Fourier transformation on 2-qudits generates the controlled transformation C_Z: $C_Z = (GF^{-1}\otimes FG^{-1})\mathfrak{F}_s(1\otimes F^{-1}G^{-1})$. Thus, $X, Y, Z, F, G, \mathfrak{F}_s$ generate the n-qudit Clifford group.

In particular, the string Fourier transformation is a topological quantum computer, as it generates any unitary transformations, along with 1-qudit transformations. This construction augments the topological model

of quantum computation [12–14, 43–45], and implies a new way to realize a universal quantum simulator [49, 52].

The pioneering work of Jozsa and Linden on the connections between quantum computational speed-ups and multipartite entanglement [73] provides further motivation to explore the role of the string Fourier transformation in quantum algorithms. In the problem of simulating physical phenomena it would be interesting to evaluate the efficiency of the string Fourier, and realize the transformation with a small-scale quantum simulator to search for the first example of a quantum advantage. See §VII of [48] for some applications of quantum simulation.

1. String Fourier transform $\mathfrak{F}_s$ for general n-qudits

In this section we show that the SFT acts on n-qudits as a unitary transformation $\mathfrak{F}_s$. We find the matrix elements $\langle \vec{\ell} | \mathfrak{F}_s | \vec{k} \rangle$ of $\mathfrak{F}_s$ in (87)–(89). We also give the matrix elements of its inverse $\mathfrak{F}_s^*$ in (90). Furthermore, we use these matrix elements to establish the fundamental relation in (92), namely that the SFT produces the maximally-entangled state from the zero-particle qudit,

$$|\text{Max}\rangle = \mathfrak{F}_s|\vec{0}\rangle = \mathfrak{F}_s^*|\vec{0}\rangle = \frac{1}{d^{\frac{n-1}{2}}} \sum_{|\vec{k}|=0} |\vec{k}\rangle . \quad (85)$$
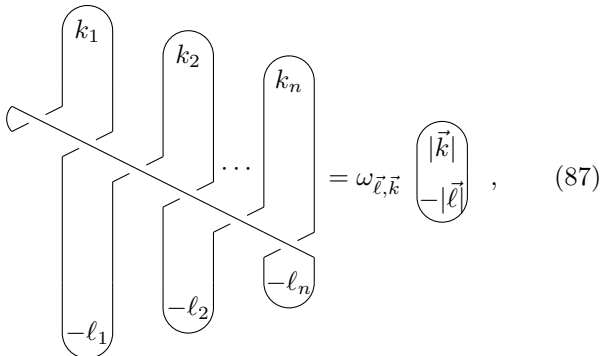
In addition, we obtain some other interesting properties of the SFT operator.

The diagram in Fig. 13 suggests that there is another formula for $\mathfrak{F}_s$ given by the braid. Let $b_{i,i+1,-}$ be the negative braid on the ith and $(i+1)^{\text{th}}$ string. Each such transformation is local. Therefore we obtain the representation of the string Fourier transformation as the local transformation on n qudits,

$$\mathfrak{F}_s = \frac{1}{\sqrt{\omega}} b_{2n-1,2n,-} \, b_{2n-2,2n-1,-} \cdots b_{1,2,-} , \quad (86)$$

with the order in the product for increasing indices from right to left.

We calculate the matrix elements $\langle \vec{\ell} | \mathfrak{F}_s | \vec{k} \rangle$ of $\mathfrak{F}_s$ in the qudit basis $|\vec{k}\rangle = |k_1, k_2, \cdots, k_n\rangle$, and the dual qudit basis $\langle \vec{\ell} | = \langle \ell_1, \ell_2, \cdots, \ell_n |$. The diagrammatic answer is given in (87), namely

$$= \omega_{\vec{\ell},\vec{k}} \begin{pmatrix} |\vec{k}| \\ -|\vec{\ell}| \end{pmatrix} , \quad (87)$$

where

$$\omega_{\vec{\ell},\vec{k}} = \zeta^{|\vec{\ell}|^2} \prod_{1 \le j_1 < j_2 \le n} q^{-\ell_{j_1} k_{j_2}} . \quad (88)$$

Thus the transformation $\mathfrak{F}_s$ can be realized as a $d^n \times d^n$ matrix, with matrix elements

$$\langle \vec{\ell} | \mathfrak{F}_s | \vec{k} \rangle = d^{\frac{1-n}{2}} \omega_{\vec{\ell},\vec{k}} \, \delta_{|\vec{\ell}|,|\vec{k}|} . \quad (89)$$

Similarly the matrix elements of the inverse string Fourier transformation on n-qudits are

$$\langle \vec{\ell} | \mathfrak{F}_s^{-1} | \vec{k} \rangle = d^{\frac{1-n}{2}} \overline{\omega}_{\vec{\ell},\vec{k}} \, \delta_{|\vec{\ell}|,|\vec{k}|} . \quad (90)$$

Moreover,

$$\mathfrak{F}_s^{2n} | \vec{k} \rangle = q^{|k|^2} | \vec{k} \rangle . \quad (91)$$

The string Fourier transform and its inverse map n-qudit product states to maximally entangled states. In particular, if $\vec{0} = (0, 0, \ldots, 0)$, we call $|\vec{0}\rangle$ the "zero particle state." Apply $\mathfrak{F}_s$ to this state, and insert (89) with $\vec{k} = \vec{0}$, to obtain the multipartite resource state,

$$|\text{Max}\rangle = \mathfrak{F}_s|\vec{0}\rangle = \sum_{\vec{\ell}} \langle \vec{\ell}|\mathfrak{F}_s|\vec{0}\rangle \, |\vec{\ell}\rangle = \frac{1}{d^{\frac{n-1}{2}}} \sum_{|\vec{k}|=0} |\vec{k}\rangle . \quad (92)$$

The coefficients of $|\vec{k}\rangle$ in the sum in (92) are all positive, because we have chosen the decreasing basis $|\vec{k}\rangle^{\searrow}$ for our qudits. Similarly $|\text{Max}\rangle = \mathfrak{F}_s^*|\vec{0}\rangle$.

We say that a protocol costs 1 n-edit, when it uses this n-qudit $|\text{Max}\rangle$ as a resource. The diagrammatic representation and the protocol for the resource state are given in Fig. 2 and 3.

K. Entropy for n-qudit entanglement

There are several possible ways to define the entanglement entropy for multi-qudits. We give one particular definition for an n-qudit density matrix ρ. Let S denote a proper subset of $\{1, 2, \ldots, n\}$ and S' its complement. Define the entanglement entropy for the set S as

$$\mathcal{E}_S(\rho) \equiv \mathcal{E}(\text{tr}_{S'}(\rho)) , \quad (93)$$

where $\mathcal{E}$ denotes the von Neumann entropy and $\text{tr}_{S'}$ denotes the partial trace on S'. This generalizes the definition in the 2-qudit case.

Then

$$\mathcal{E}_S(\rho_{\text{Max}}) = -\frac{1}{d^{|S|}} \ln \frac{1}{d^{|S|}} , \quad (94)$$

where ρ_{Max} is the density matrix corresponding to the state $|\text{Max}\rangle$. We call our state Max, since it achieves the maximal entanglement entropy among the set of pure states.

L. The resource states |Max⟩ and |GHZ⟩

Here we establish the relation stated in (6), between the maximally-entangled resource state |Max⟩ and |GHZ⟩. In particular, these states are the ordinary Fourier transform $F \otimes \cdots \otimes F$ of one-another. To see this, use the representation (92) for |Max⟩. Then

$$(F \otimes \cdots \otimes F)|\text{Max}\rangle = \frac{1}{d^{\frac{n-1}{2}+\frac{n}{2}}} \sum_{\substack{\vec{\ell} \\ \vec{k}:k_n=-k_1-\cdots-k_{n-1}}} q^{\vec{k}\cdot\vec{\ell}}|\vec{\ell}\rangle \ .$$
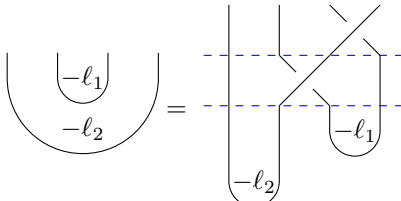
Carry out the $(n-1)$ sums over $k_1,\ldots,k_{n-1}$ for fixed $\vec{\ell}$. These sums vanish unless $\ell_j = \ell_n$, for each $j = 1,\ldots,n-1$. In case all the equalities hold, there are d^{n-1} equal, non-zero terms. Thus the answer is as claimed in (6), namely

$$(F \otimes \cdots \otimes F)|\text{Max}\rangle = \frac{1}{d^{\frac{1}{2}}} \sum_\ell |\ell,\ldots,\ell\rangle = |\text{GHZ}\rangle \ . \quad (95)$$
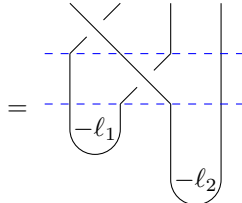
The same result would arise with F^{-1} in place of F.

Up to a unitary equivalence, |Max⟩ and |GHZ⟩ are the same state. But we prefer the state |Max⟩ as the resource state for n-qudits, rather than |GHZ⟩, because |Max⟩ both has a *topological interpretation*, and in addition it is *neutral*.

M. Measurement dictionary II

$$(96)$$

$$(97)$$

We give a dual 2-qudit as a double-cup diagram in (96), (97). The two corresponding protocols are given in Fig. 15, 16 depending on the choice of the control qudit. They are equivalent to the protocol for measurement in phase space.
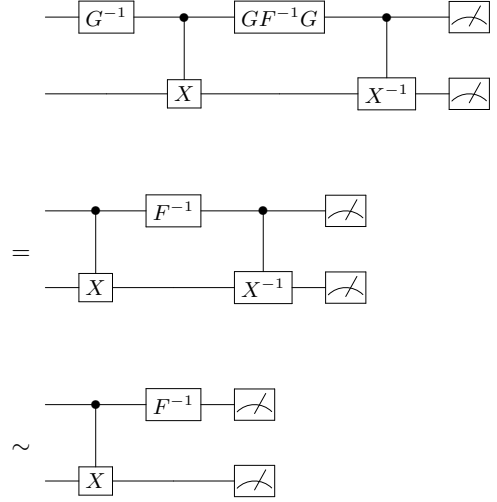

FIG. 15. Measurement in the phase space: The first protocol is translated from the double-cup diagram on the right of (96), where the measurement of the first and the second meters are ℓ_1 and ℓ_2 respectively. It is simplified as the second protocol using tricks in Figs. 8, 9. It is equivalent to the measurement in the phase space using the trick in Fig. 10.
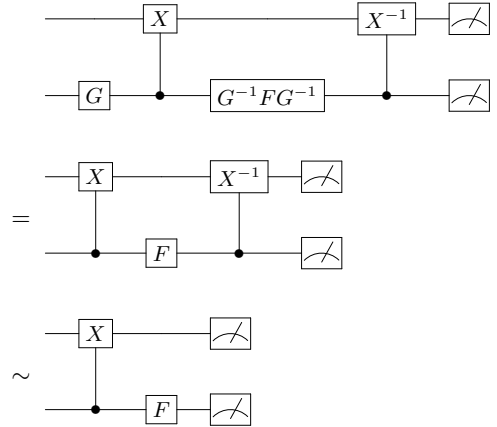

FIG. 16. Measurement in the phase space. This protocol is a translation of (97).

IV. DIAGRAMMATIC IDENTIFICATION FOR PROTOCOLS

Now we complete the dictionary of our holographic software. We can use this dictionary to translate diagrammatic protocols to algebraic ones.

In this section we illustrate the robustness of the diagrammatic method, by giving examples. We identify the standard teleportation protocol. As mentioned in the introduction, in a separate paper we present the new compressed teleportation (CT) protocol.

Here we also construct a protocol to produce the multipartite entangled resource state |Max⟩ for n persons.

This protocol requires using $(n-1)$ usual 2-edits, and $(n-1)$ cdits. This cost is minimal, as is the cost in time, which is the transmission of one cdit.

When we translate between a diagrammatic realization of a protocol and an algebraic realization of that protocol, an overall (global) phase is irrelevant. It does not affect a quantum-mechanical vector state, even though in this paper we often do keep track of this phase.

A. Teleportation

The diagram for standard qudit teleportation is

$$(98)$$

$$(99)$$

$$(100)$$
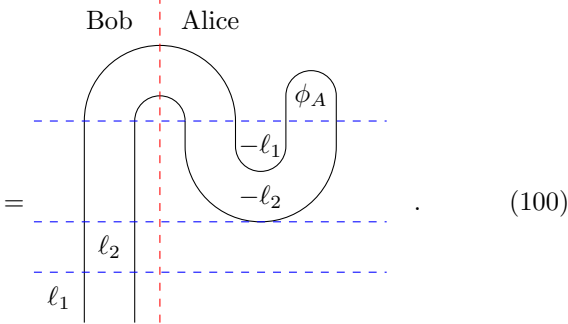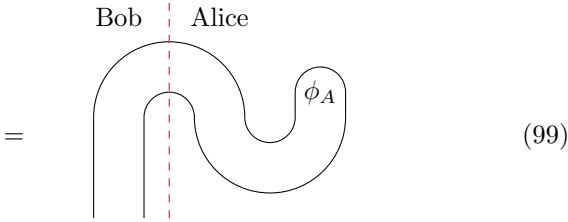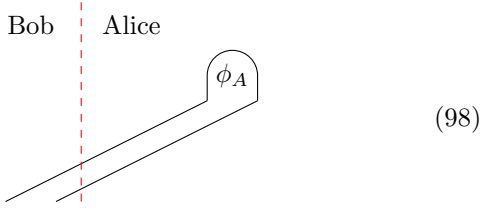
In (99), we regularize the diagram, so that the string across the dotted line is the resource state $|\text{Max}\rangle$. In (100), we add charges $-\ell_1, -\ell_2$ to the double-cup dual qudit. (That means Alice measures the qudits by the meters and the measurements are ℓ_1 and ℓ_2.) Moreover, we make up ℓ_1, ℓ_2 on the corresponding strings. (That means Alice transmits the cdits to Bob, and Bob applies the corresponding transformations.)

Using our dictionary, we can translate the diagrammatic protocol in (100) piecewise to an algebraic protocol illustrated in Fig. 17. When $d = 2$, it is exactly the original qubit teleportation protocol.
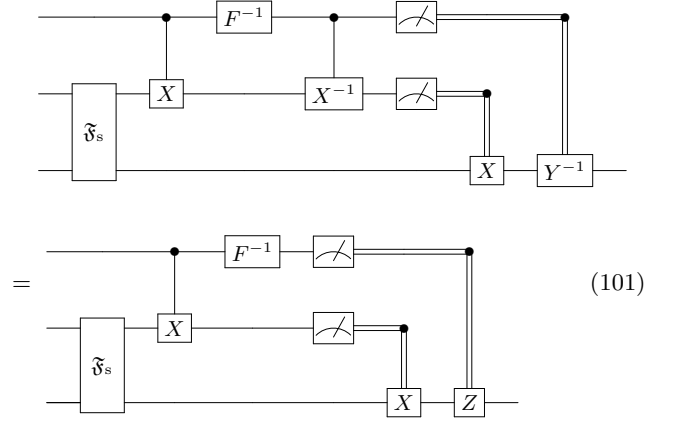

$$(101)$$

FIG. 17. Teleportation protocol: Measurement in the phase space: The first protocol represents the holographic translation of the diagrammatic protocol (100). It can be simplified to the protocol (101) using tricks in Figs. 10 and 11.
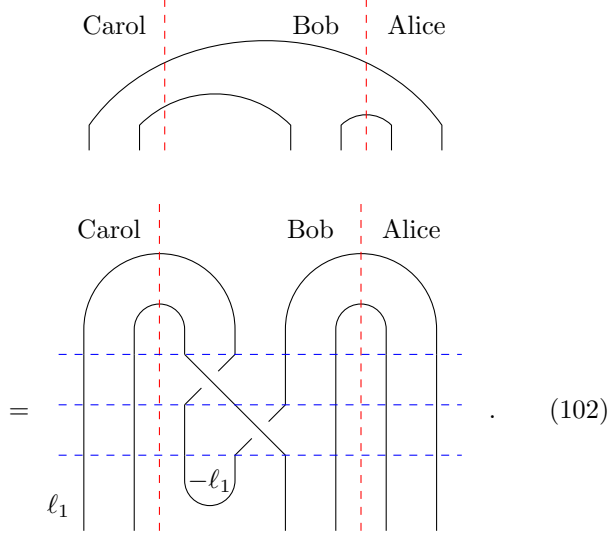
B. Multipartite resource state

We introduce the multipartite entangled resource state in (92). We can construct this n-qudit resource state using $(n-1)$ of the 2-qudit resource states. We give the diagrammatic protocol in (102) and the algebraic protocol in Fig. 18 for the case $n = 3$. One can easily generalize the protocol to the case for arbitrary n.

For the case $n = 3$ this entanglement protocol indicates how to construct a corresponding swapping protocol. It also shows that the usual swapping protocol wastes entanglement.

The point is that the usual swapping protocol uses the resource state between Alice and Bob, as well as the resource state between Bob and Carol. The result is a resource state between Alice and Carol. However, using our protocol we construct one resource state among the three persons: Alice, Bob, and Carol. In this way we do not lose the entanglement between Alice and Bob or between Bob and Carol. We can recover the resource state between one pair by measuring the qudit of the third person.

Our protocol for constructing the multipartite entangled resource state costs minimal edits. However, it is better to construct the multipartite entangled resource state as quantum software [30, 74] at a station and teleport each component to one person by a noiseless channel. This uses n noiseless channels in total. On the other hand, the construction of $(n-1)$, 2-qudit resource states uses $2(n-1)$ noiseless channels. Therefore, one may save cost by using n-qudit resource states for multipartite communication. Actually, it does save 50% in our new protocol given in [23].

$$= \qquad . \qquad (102)$$

FIG. 18. The construction of the n-edit resource for $n = 3$.

C. The BVK protocol

Here we give a more general construction of $|\text{Max}\rangle$ for a multipartite network, motivated by the Bose-Vedral-Knight protocol [21], and the challenge of Kimble to entangle nodes across a network for a quantum internet [22]. Suppose there are n parties and the jth party has n_j persons with a shared multipartite entangled resource state $|\text{Max}\rangle$. In each party there is one leader who shares an extra multipartite entangled resource state $|\text{Max}\rangle$. Then we can construct a multipartite entangled resource state $|\text{Max}\rangle$ for all members among the n parties. We illustrate this situation with a diagrammatic protocol in (103). We illustrate the corresponding algebraic protocol in Fig. 19.

V. CONCLUSION

We relate holographic software to communication. We have given a comprehensive dictionary to translate back and forth between algebraic protocols and diagrammatic software. We found new protocols in this way. It would be interesting to relate quantum information algorithms, such as [75], to these ideas.

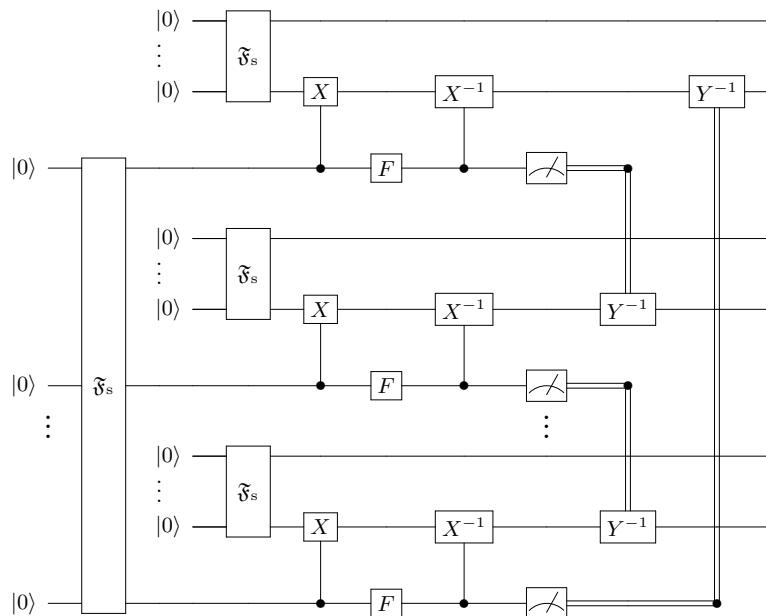$$= \prod_{j=2}^{n} \zeta^{l_j^2} \qquad (103)$$
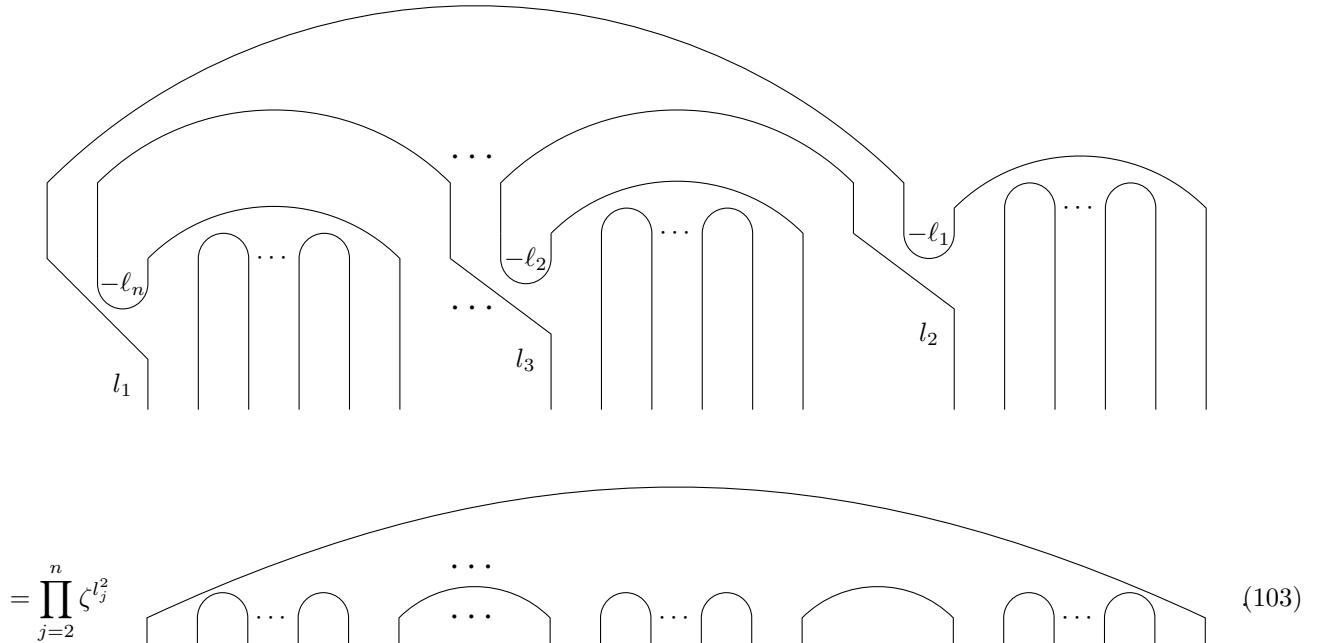
FIG. 19. The algebraic protocol for the iterated construction of the multipartite entangled resource state for multipartite communication corresponding to the diagram in (103).

[1] Yu. Manin, Computable and uncomputable (book in Russian). Moscow, Sovetskoye Radio, 1980.

[2] R. Feynman, Simulating physics with computers, *International Journal of Theoretical Physics* **21**, (1982), Issue 6, 467–488, doi:10.1007/BF02650179.

[3] Yu. Manin, Classical computing, quantum computing, and Shor's factoring algorithm, Séminaire Bourbaki, no. 862 (June 1999), *Astérisque*, vol 266, (2000), 375–404, https://arxiv.org/abs/quant-ph/9903008.

[4] C. H. Bennett, G. Brassard, C. Crépeau, R. Jozsa, A. Peres, and W. K. Wooters, Teleporting an unknown quantum state via dual classical and Einstein-Podolsky-Rosen Channels, *Phys. Rev. Lett.* **70**, (1993) 1895, doi:10.1103/PhysRevLett.70.1895.

[5] V. F. R. Jones, Index for subfactors, *Invent. Math.* **72** (1983), 1–25, http://link.springer.com/article/10.1007%2FBF01389127?LI=true.

[6] V. F. R. Jones, A polynomial invariant for links via von Neumann algebras, *Bull. Amer. Math. Soc.* **12** (1985), 103–111, http://www.ams.org/journals/bull/1985-12-01/S0273-0979-1985-15304-2/S0273-0979-1985-15304-2.pdf.

[7] V. F. R. Jones, Hecke algebra representations of braid groups and link polynomials, *Ann. of Math* **126** (1987), no. 2, 335–388, doi:10.2307/1971403.

[8] E. Witten, Topological quantum field theory, *Comm. Math. Phys.* **117** (1988), no. 3, 353–386. doi:10.1007/BF01223371

[9] M. F. Atiyah, Topological quantum field theories, Publications Mathématiques de l'IHÉS **68** (1988), 175–186, doi:10.1007/BF02698547.

[10] N. Reshetikhin and V. Turaev, Invariants of 3-manifolds via link polynomials and quantum groups, *Invent. Math.* **103** (1991), 547–597, doi:10.1007/BF01239527

[11] V. Turaev and O. Ya. Viro, State sum invariants of 3-manifolds and quantum $6j$-symbols, *Topology* **31** (1992), 865–902, doi:10.1016/0040-9383(92)90015-A

[12] A. Kitaev, Fault-tolerant quantum computation by anyons, *Ann. Phys.* **303** (2003), 2–30, arXiv:quant-ph/9707021, doi:10.1016/S0003-4916(02)00018-0.

[13] M. H. Freedman, A. Kitaev, M. J. Larsen, and Z. Wang, Topological quantum computation, *Bulletin of the American Mathematical Society* Volume 40, Number 1, (2002), 31–38, doi:10.1090/S0273-0979-02-00964-3.

[14] M. H. Freedman, A. Kitaev, and Z. Wang, Simulation of topological field theories by quantum computers, *Commun. Math. Phys.*, **227** (2002), 587–603, doi:10.1007/s002200200635.

[15] D. Deutsch, Quantum computational networks, *Proceedings of the Royal Society of London. Series A, Mathe-*

matical and Physical Sciences, Vol. 425, No. 1868 (1989), 73–90, doi:10.1098/rspa.1989.0099.

[16] L. Kauffman and S. Lomonaco Jr., Braiding operators are universal quantum gates, *New J. Phys.* **6** (2004) 134, doi:10.1088/1367-2630/6/1/134.

[17] B. Coecke, Quantum picturalism, *Contemporary Physics*, **51:1** (2010), 59–83, http://www.tandfonline.com/doi/pdf/10.1080/00107510903257624

[18] S. Abramsky and B. Coecke. A categorical semantics of quantum protocols, *Logic in Computer Science, 2004. Proceedings of the 19th Annual IEEE Symposium* IEEE (2004).

[19] B. Coecke and A. Kissinger, Picturing quantum processes: A first course in quantum theory and diagrammatic reasoning, Cambridge University Press, to be published.

[20] A. M. Jaffe and Z. Liu, Planar para algebras, reflection positivity, preprint, http://arxiv.org/abs/1602.02662.

[21] S. Bose, V. Vedral, and P. L. Knight, Multiparticle generalization of entanglement swapping, *Phys. Rev. A* **57**, (1998) 822–829, doi:10.1103/PhysRevA.60.194.

[22] H. J. Kimble, The quantum internet, *Nature* **453** (2008), 1023–1030, doi:10.1038/nature07127.

[23] A. M. Jaffe, Z. Liu, and A. Wozniakowski, Compressed teleportation, https://arxiv.org/abs/1605.00321.

[24] J-W. Pan, Quantum science satellite, *Chin. J. Space Sci.* **34** (2014), 547–549, doi:10.11728/cjss2014.05.547.

[25] C. Biever, China's quantum space pioneer: We need to explore the unknown, *Nature*, doi:10.1038/nature.2016.19166.

[26] D. M. Greenberger, M. A. Horne, and A. Zeilinger, Going beyond Bell's theorem, http://arxiv.org/abs/0712.0921 in *Bell's theorem, quantum theory, and conceptions of the universe*, M. Kafakos, editor, Vol. 37 of "Fundamental Theories of Physics," Springer Verlag, Heidelberg (1989), doi:10.1007/978-94-017-0849-4.

[27] M. Żukowski, A. Zeilinger, M. A. Horne, and A. K. Ekert, "Event-ready-detectors" Bell experiment via entanglement swapping, *Phys. Rev. Lett.* **71**, (1993) 4287–4290, doi:10.1103/PhysRevLett.71.4287.

[28] M. A. Nielsen and I. L. Chuang, Programmable quantum gate arrays, *Phys. Rev. Lett.* **79**, (1997) 321, doi:10.1103/PhysRevLett.79.321.

[29] A. Sørensen and K. Mølmer, Error-free quantum communication through noisy channels, *Phys. Rev. A.* **58**, (1998) 2745, doi:10.1103/PhysRevA.58.2745.

[30] D. Gottesman and I. L. Chuang, Demonstrating the viability of universal quantum computation using teleportation and single-qubit operations, *Nature* **402**, (1999) 390–393, doi:10.1038/46503.

[31] P. van Loock and S. L. Braunstein, Multipartite entanglement for continuous variables: a quantum teleportation network, *Phys. Rev. Lett.* **84**, (2000) 3482, doi:10.1103/PhysRevLett.84.3482.

[32] X. Zhou, D. W. Leung, and I. L. Chuang, Methodology for quantum logic gate construction, *Phys. Rev. A* **62**, (2000) 052316, doi:10.1103/PhysRevA.62.052316.

[33] J. Eisert, K. Jacobs, P. Papadopoulos, and M. B. Plenio, Optimal local implementation of nonlocal quantum gates, *Phys. Rev. A* **62**, (2000) 052317, doi:10.1103/PhysRevA.62.052317.

[34] S. F. Huelga, J. A. Vaccaro, A. Chefles, and M. B. Plenio, Quantum remote control: teleportation of unitary operations, *Phys. Rev.* **A 63**, (2001) 042303, doi:10.1103/PhysRevA.63.042303.

[35] B. Reznik, Y. Aharonov, and B. Groisman, Remote operations and interactions for systems of arbitrary-dimensional hilbert space: state-operator approach, *Phys. Rev.* **A 65**, (2002) 032312, doi:10.1103/PhysRevA.65.032312.

[36] N. B. Zhao and A. M. Wang, Hybrid protocol of remote implementations of quantum operations, *Phys. Rev.* **A 76**, (2007) 062317, doi:10.1103/PhysRevA.76.062317.

[37] M. A. Nielsen and I. L. Chuang, Quantum computation and quantum information, Cambridge University Press, 10th Anniversary Edition, 2010.

[38] L. Yu, R. B. Griffiths, and S. M. Cohen, Efficient implementation of bipartite nonlocal unitary gates using prior entanglement and classical communication, *Phys. Rev.* **A 81**, (2010) 062315, doi:10.1103/PhysRevA.81.062315.

[39] S. Luo and A. M. Wang, Remote implementations of partially unkown quantum operations and its entanglement costs, (2013), http://arxiv.org/pdf/1301.5866.pdf.

[40] R. Van Meter, Quantum Networking, John Wiley & Sons, 2014.

[41] S. Hu, W.-X. Cui, D.-Y. Wang, C.-H. Bai, Q. Guo, H.-F. Wang, A.-D. Zhu, and S. Zhang, Teleportation of a Toffoli gate among distant solid-state qubits with quantum dots embedded in optical microcavities, *Nature: Scientific Reports* **5** (2015) 11321, doi:10.1038/srep11321.

[42] A. Hutter and D. Loss, Quantum computing with parafermions, *Phys. Rev.* **B 93**, (2016) 125105 1–7, doi:10.1103/PhysRevB.93.125105.

[43] R. Ogburn and J. Preskill, Topological quantum computation, *Quantum computing and quantum communications*, **1509** (1999), 341–356, doi:10.1007/3-540-49208-9˙31.

[44] H. Bombin and M. A. Martin-Delgado, Topological computation without braiding, *Phys. Rev. Lett.* **B 98**, (2007) 160502, doi:10.1103/PhysRevLett.98.160502.

[45] C. Nayak, S. H. Simon, A. Stern, M. Freedman, and S. Das, Non-Abelian anyons and topological quantum computation, *Rev. Mod. Phys.* **B 80**, (2008) 1083, doi:10.1103/RevModPhys.80.1083.

[46] E. Candès, J. Romberg, and T. Tao, Robust uncertainty principles: exact signal reconstruction from highly incomplete frequency information, *IEEE Transactions on Information Theory* **52** (2006), 489–509. doi:10.1109/TIT.2005.862083

[47] J. Ignacio and P. Zoller, Goal and opportunities in quantum simulation, *Nature Physics* **8** (2012) 264–266, doi:10.1038/nphys2275.

[48] I. M. Georgescu, S. Ashhab, and F. Nori, Quantum simulation, *Rev. Mod. Phys.* **86** (2014) 153, doi:10.1103/RevModPhys.86.153.

[49] S. Lloyd, Universal quantum simulators, *Science* **273** (1996) 1073–1078, doi:10.1126/science.273.5278.1073.

[50] C. Zalka, Efficient simulation of quantum systems by quantum computers, *Proceedings of the Royal Society of London. Series A, Mathematical and Physical Sciences*, Vol. 454, No. 1969 (1998), doi:10.1098/rspa.1998.0162.

[51] D. Abrams and S. Lloyd, Simulation of many-body fermi systems on a universal quantum computer, *Phys. Rev. Lett.* **79** (1997) 2586, doi:10.1103/PhysRevLett.79.2586.

[52] R. Somma, G. Ortiz, J. E. Gubernatis, E. Knill, and R. Laflamme, Simulating physical phenomena by quan-

tum networks, *Phys. Rev.* **A 65** (2002) 042323, doi: 10.1103/PhysRevA.65.042323.

[53] I. Buluta and F. Nori, Quantum simulators, *Science* **326** (2009) 108–111, doi:10.1126/science.1177838.

[54] A. Trabesinger, Quantum simulation, *Nature Physics* **8** (2012) 263, doi:10.1038/nphys2258.

[55] I. Bloch, J. Dalibard, and S. Nascimbène, Quantum simulations with ultracold quantum gases, *Nature Physics* **8** (2012) 267–276, doi:10.1038/nphys2259.

[56] R. Blatt and C. F. Roos, Quantum simulations with trapped ions, *Nature Physics* **8** (2012) 277–284, doi: 10.1038/nphys2252.

[57] A. Aspuru-Guzik and P. Walther, Photonic quantum simulations, *Nature Physics* **8** (2012) 285–291, doi: 10.1038/nphys2253.

[58] A. Houck, H. Türeci, and J. Koch, On-chip quantum simulation with superconducting circuits, *Nature Physics* **8** (2012) 292–299, doi:10.1038/nphys2251.

[59] D. Gottesman, The Heisenberg representation of quantum computers, *Talk at International Conference on Group Theoretic Methods in Physics* (1998), http://arxiv.org/pdf/quant-ph/9807006v1.pdf.

[60] G. Vidal, Efficient classical simulation of slightly entangled quantum computations, *Phys. Rev. A* **70**, (2004) 052328, doi:10.1103/PhysRevLett.91.147902.

[61] S. Aaronson and D. Gottesman, Improved simulation of stabilizer circuits, *Phys. Rev. Lett.* **91**, (2003) 147902, doi:10.1103/PhysRevA.70.052328.

[62] A. M. Jaffe and F. L. Pedrocchi, Reflection positivity for parafermions, *Commun. Math. Phys.*, **337** (2015), 455–472, doi:10.1007/s00220-015-2340-x.

[63] A. M. Jaffe and B. Janssens, Characterization of reflection positivity, *Commun. Math. Phys.*, (2016), doi: 10.1007/s00220-015-2545-z.

[64] V. F. R. Jones, Baxterization, *Inter. J. Modern Physics A* **6** (1991), no. 12, 2035–2043, doi: 10.1142/S0217751X91001027.

[65] R. Baxter, Eight-vertex model in lattice statistics and one-dimensional anisotropic Heisenberg chain I, II, III, *Ann. Phys.* **76** (1973), 1–24, 25–47, 48–71, doi:10.1016/0003-4916(73)90439-9, doi:10.1016/0003-4916(73)90440-5, doi:10.1016/0003-4916(73)90441-7.

[66] C. N. Yang, Some exact results for the many-body problem in one dimension with repulsive delta-function interaction, *Phys. Rev. Lett.*, **19** (1967), 1312–1315, doi: 10.1103/PhysRevLett.19.1312.

[67] V. Fateev and A. B. Zamolodchikov, Self-dual solutions of the star-triangle relations in $\mathbb{Z}_N$-models, *Physics Letters* **92A** (1982), 37–39, doi:10.1016/0375-9601(82)90736-8.

[68] J. Fröhlich, New super-selection sectors ("Soliton-States") in two-dimensional Bose quantum field models, *Commun. Math. Phys.* **47** (1976), 269–310, http://projecteuclid.org/download/pdf_1/euclid.cmp/1103899761.

[69] J. Fröhlich, Statistics of fields, the Yang-Baxter equation, and the theory of knots and links, in *Non-Perturbative Quantum Field Theory*, G. 't Hooft et al. (eds.) New York, Plenum Press 1988, doi:10.1007/978-1-4613-0729-7˙4.

[70] J. Schliemann, D. Loss, A. H. MacDonald, Double-occupancy errors, adiabaticity, and entanglement of spin qubits in quantum dots, *Phys. Rev. B* **63** (2001), 085311, doi:10.1103/PhysRevB.63.085311.

[71] J. Schliemann, J. Ignacio Cirac, M. Kuś, M. Lewenstein, and D. Loss, Quantum correlations in two-fermion systems, *Phys. Rev. A* **64**, (2001) 022303, doi: 10.1103/PhysRevA.64.022303.

[72] C. Jiang, Z. Liu and J. Wu, Noncommutative uncertainty principles, *Jour. Funct. Anal.* **270.1** (2016), 264–311, doi:10.1016/j.jfa.2015.08.007.

[73] R. Jozsa and N. Linden, On the role of entanglement in quantum computational speed-up, *Proceedings of the Royal Society of London. Series A, Mathematical and Physical Sciences*, Vol. 459, No. 2036 (2003), doi: 10.1098/rspa.2002.1097.

[74] J. Preskill, Plug-in quantum software, *Nature* **402** (1999) 357–358, doi:10.1038/46434.

[75] P. Shor, Algorithms for quantum computation: discrete logarithms and factoring, *Foundations of Computer Science, 1994 Proceedings, 35th Annual IEEE Symposium.* doi:10.1109/SFCS.1994.365700.